Non-Gaussian dynamics in smectic liquid crystals of parallel hard rods

Rik Matena, Marjolein Dijkstra,* and Alessandro Patti†
Soft Condensed Matter, Debye Institute for NanoMaterials Science, Utrecht University, Princetonplein 5, 3584 CC Utrecht, The Netherlands

(Received 14 October 2009; published 16 February 2010)

Using computer simulations, we studied the diffusion and structural relaxation in *equilibrium* smectic liquid-crystal bulk phases of parallel hard spherocylinders. These systems exhibit a non-Gaussian layer-to-layer diffusion due to the presence of periodic barriers and transient cages and show remarkable similarities with the behavior of *out-of-equilibrium* supercooled liquids. We detect a very slow interlayer relaxation dynamics over the whole density range of the stable smectic phase which spans a time interval of four time decades. The intrinsic nature of the layered structure yields a hopping-type diffusion which becomes more heterogeneous for higher packing fractions. In contrast, the in-layer dynamics is typical of a dense fluid with a relatively fast decay. Our results on the dynamic behavior agree well with that observed in systems of freely rotating hard rods but differ quantitatively as the height of the periodic barriers reduces to zero at the nematic-smectic transition for aligned rods, while it remains finite for freely rotating rods.

DOI: 10.1103/PhysRevE.81.021704 PACS number(s): 61.30.−v, 82.70.Dd, 87.15.Vv

I. INTRODUCTION

Non-Gaussian diffusion and dynamical heterogeneities have been shown to slow down or completely arrest the structural relaxation of systems, such as supercooled liquids [1–3] and gels [4,5]. The heterogeneous dynamics of these systems, in which individual particles are trapped in transient cages by neighboring particles, explains the nonexponential relaxation and non-Gaussian diffusive behavior. Two scenarios are usually proposed to explain the nonexponential relaxation behavior: a *heterogeneous scenario* in which the particles relax exponentially at different relaxation rates and a *homogeneous scenario* where the particles relax nonexponentially at nearly identical rates [6]. Recently, the analysis of dynamical heterogeneities has been extended to other complex systems, such as granular media [7] and liquid crystals (LCs) in confined nanopores [8,9]. Interestingly, the dynamics of LCs has been shown to share many features with supercooled liquids, especially in the so-called LC isotropic phase [10,11] and in the smectic LC phase [12]. The LC isotropic phase is a macroscopically homogeneous liquid phase, which exhibits nematic ordered domains near the isotropic-nematic (IN) transition. The size of these nematic domains, which are driven by a precursor of the nematic phase, increases upon approaching the IN transition [13]. The caging behavior, i.e., the temporary localization of individual particles, as observed in supercooled liquids, is caused by the transient structural inhomogeneities of the nematic domains in the isotropic LC phase. Hence, the heterogeneous dynamics of such an isotropic phase with prenematic order resembles that of supercooled liquids [10]. The non-Gaussian behavior becomes even stronger by confining the LC in a nanoporous material [8,9]. The reason is that confinement modifies the dynamics of the LC particles, which yields a nonuniform relaxation depending on, e.g., the distance to the pore surface and the pore size, which is indeed observed experimentally by dielectric spectroscopy [14] and quasielastic neutron scattering [8,15].

For the bulk smectic LCs, recent developments of experimental techniques (e.g., NMR coupled to strong magnetic field gradients [16] or fluorescent labeling of rods [17]) allowed for direct observations of non-Gaussian quasiquantized layer-to-layer diffusion. In particular, Lettinga and Grelet found that the interlayer diffusion of rodlike *fd* viruses (aspect ratio $\simeq$130) in smectic phases is faster than the layer-to-layer one [17]. In the light of these advances, Bier *et al.* proposed a dynamic density functional approach to study the self-diffusion in colloidal dispersions of infinitely elongated particles [18]. In particular, they investigated the effect of the local fluid structure, which temporarily cages individual particles and competes with the one-dimensional "permanent" barriers due to the smectic layered structure. This theoretical work shows qualitative agreement with recent experiments on the self-diffusion of filamentous bacteriophage *fd* viruses through smectic layers [17]. In both studies, the self-part of the van Hove correlation function showed clear evidence of an interlayer diffusion (or *permeation*) occurring by discontinuous jumps of nearly one rod length. Simulations on freely rotating hard rods confirmed the important role of temporary cages and permanent barriers on the non-Gaussian permeation through smectic layers and revealed insights on the relaxation behavior and cooperative motion of stringlike clusters [12]. However, the simulations did not show a faster layer-to-layer diffusion compared with the in-layer diffusion as found in the experiments on *fd* virus particles [17]. This might be explained by the huge aspect ratio of *fd* virus, while the simulations were performed on relatively short rods.

In this work, we investigate the diffusion in bulk smectic liquid crystals of perfectly aligned hard spherocylinders. The phase diagram of parallel hard spherocylinders exhibit nematic-to-smectic (N-Sm) and smectic-to-crystal (Sm-K) phase transitions in a broad range of length-to-diameter ratios of the rods [19,20]. Using computer simulations, we are able to study the long-time relaxation decay which approxi-

*m.dijkstra1@uu.nl
†a.patti@uu.nl

mately spans up to four time decades in the whole density range from the N-Sm to the Sm-K transition. We investigate the substantial differences between the fluidlike in-layer and the hopping-type interlayer dynamics, which are caused by the temporary cages and permanent barriers. In addition, we study the heterogeneous character of the layer-to-layer dynamics, which is not exclusively a feature of confined LCs, and we determine the crossover between the cage regime, with the particles rattling around their center of mass, and the long-time diffusive regime as a function of density.

II. MODEL AND SIMULATIONS

Our system is composed of $N=2100$ parallel hard spherocylinders with aspect ratio $L^* \equiv L/D=5$, where D is the diameter of the hemispherical caps joined together by a cylindrical part of length L. Hence, the overall length of the rods is $L+D$. The phase diagram of this system displays stable nematic, smectic, and crystal phases [20]. For $L^*=5$, the smectic phase melts into a nematic phase for $P^* \lesssim 2.1$, and crystallizes for $P^* \gtrsim 6.3$, where $P^* \equiv P v_0 / k_B T$ is the reduced pressure with k_B Boltzmann's constant and $v_0=\pi(D^3/6+LD^2/4)$ the molecular volume. We studied the dynamics of this system at pressures $P^*=2.0$, 2.5, 3.0, 4.0, and 5.0 corresponding to packing fractions $\eta=Nv_0/V=0.394$, 0.441, 0.475, 0.525, and 0.563, respectively. We performed Monte Carlo (MC) simulations in a rectangular box of volume V with seven smectic layers of aligned rods and we employ periodic boundary conditions.

We first performed equilibration runs using MC simulations in the isobaric-isothermal (NPT) ensemble. The initial configurations for the smectic phase were obtained by expanding a solid phase at pressures $P^*=2.0$, 2.5, 3.0, and 4.0. The smectic phase at $P^*=5.0$ was obtained by a compression run from $P^*=4.0$. We only performed translational moves, which were accepted if no overlap was detected, whereas rotational moves were not allowed. Volume changes have been attempted every N MC cycles by randomly changing the three box lengths independently. The systems were considered to be equilibrated when the packing fraction had reached a constant value. In the production runs, we carried out MC simulations in the canonical (NVT) ensemble, i.e., we kept the volume constant, as the collective moves associated with the volume changes would not correspond with Brownian dynamics. The maximum displacement of the MC moves was chosen in such a way that we achieve (i) a reasonable time of simulation, (ii) a satisfactory acceptance rate, and (iii) a suitable description of the Brownian motion of the particles in a colloidal suspension. To this end, we monitored the mean-square displacement in the z and xy directions for several values of the maximum step size δ_{max}, with $\delta_{max,z}=2\delta_{max,xy}$ due to the anisotropy of the short-time self-diffusion coefficient of the rods [21]. $\delta_{max,xy}=D/10$ and $\delta_{max,z}=D/5$ were found to be the optimal values satisfying the above requirements. We have neglected the hydrodynamic effects as it was shown recently by computer simulations of highly concentrated rod suspensions that the dynamics is dominated primarily by the excluded volume and steric effects [22].

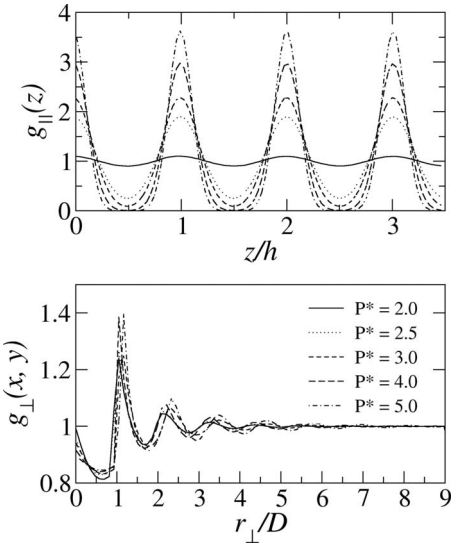

FIG. 1. (top) Interlayer $g_{\parallel}(z)$ and (bottom) in-layer $g_{\perp}(x,y)$ pair-correlation functions as a function of z and $r_{\perp}=\sqrt{x^2+y^2}$, respectively, for varying pressures as labeled.

As unit of time, we have chosen $\tau \equiv D^2/D_{tr}$, where D_{tr} is the translational short-time diffusion coefficient, which is the isotropic average of the diffusion coefficients in the three space dimensions: $D_{tr} \equiv (D_{\parallel}+2D_{\perp})/3$. At short times, when the single particle is rattling around its original position and does not yet feel the presence of the surrounding cage, the dependence of D_{tr} on the reduced pressure is very weak and can be safely neglected.

III. RESULTS

The intrinsic nature of the smectic phases can be appreciated by computing the in-layer $g_{\perp}(x,y)$ and interlayer $g_{\parallel}(z)$ pair-correlation functions as a function of $r_{\perp}=\sqrt{x^2+y^2}$ and z, respectively. In Fig. 1, we display $g_{\perp}(x,y)$ and $g_{\parallel}(z)$ for varying pressures. We find features of fluidlike behavior for $g_{\perp}(x,y)$: the first peak is located at a distance approximately equal to one diameter length and an exponential decay of the oscillations to one at long distances. By contrast, $g_{\parallel}(z)$ shows pronounced periodic correlations which reveal the layered structure along the nematic director $\hat{n}$. The location of the peaks corresponds to the center of the smectic layers, where the particle density is maximal. In Fig. 2, we show the top and side view of two typical configurations of the smectic LC phase at $P^*=2.5$ and 5.0, where one can clearly see the periodic structure of the smectic layers and the two-dimensional (2D) fluidlike structure within each layer.

Upon increasing the pressure, the peaks become more pronounced indicating that the smectic layers are more well defined and the layer spacing reduces significantly from $h=7.03D$ at $P^*=2.0$ to $h=6.48D$ at $P^*=5.0$. At $P^*=2.0$, very close to the N-Sm transition, it is difficult to distinguish the individual layers as the amplitude of the periodic structure reduces continuously, and $g_{\parallel}(z)$ approaches a nearly flat profile in the proximity of the continuous N-Sm transition. At pressures $P^* \geq 4.0$, the peaks become more pronounced,

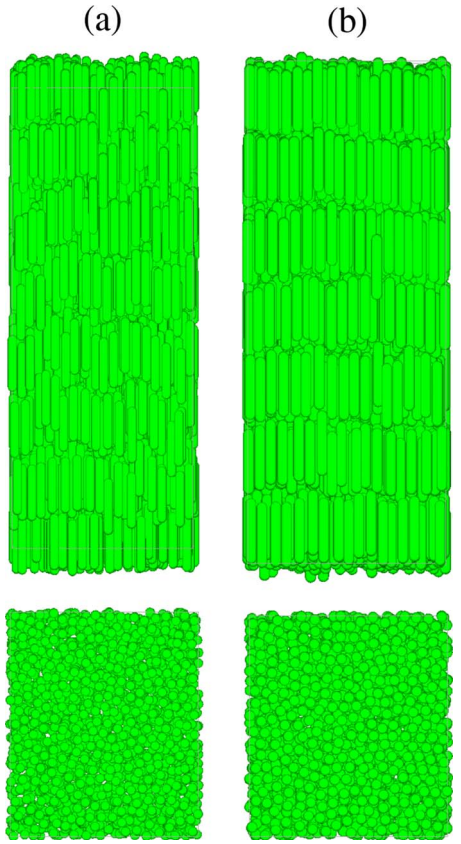

FIG. 2. (Color online) Top and side views of two bulk smectic liquid-crystal phases observed at (a) $P^*=2.5$ and (b) $P^*=5.0$.

while the minima corresponding to the interlayer spacings tends to zero. Hence, it becomes more difficult for the particles to diffuse from layer to layer at these high pressures.

In addition, we measure the (relative) probability $\pi(z)$ of finding a particle at position z with the z axis chosen parallel to the nematic director $\hat{n}$. We estimated the potential-energy barrier from the Boltzmann factor $\pi(z) \propto \exp[-U(z)/k_BT]$ as in Ref. [17]. $U(z)$ denotes the effective potential and quantifies the potential-energy barrier for the layer-to-layer diffusion. In Fig. 3, we give $U(z)$ at different pressures with the fitting function $U(z)=\Sigma_{i=1}^{n} U_i[\sin(\pi z/h)]^{2i}$, where $U_0=\Sigma_{i=1}^{n} U_i$ is the potential barrier height and h is the interlayer spacing. We find $U_0=0.2k_BT$ at $P^*=2.0$ and

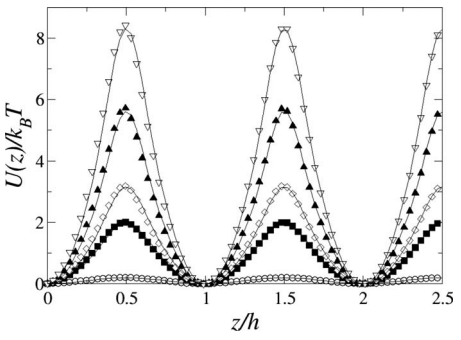

FIG. 3. Effective potential $U(z)$ in the bulk smectic phase at $P^*=2.0$ (○), 2.5 (■), 3.0 (◇), 4.0 (▲), and 5.0 (▽). The solid lines are fits.

$U_0=8.3k_BT$ at $P^*=5.0$. The potential barrier for a rod to diffuse from layer to layer increases with increasing packing fraction and becomes less steep when the N-Sm phase transition is approached at lower densities. A similar trend was observed in Ref. [17], where the height of the potential barrier increases from $0.66k_BT$ to $1.36k_BT$ by decreasing the ionic strength. This is most probably due to the fact that at low ionic strength there might be a stronger correlation between the particles, which give rise to a denser packing. We note that potential-energy barriers of $\sim 1-4k_BT$ were measured experimentally in thermotropic liquid crystals [23,24].

Our results should be compared with those of Ref. [25] and the barrier heights estimated recently for smectic phases of freely rotating hard rods with $L^*=5$, where the nematic order parameter was defined as $S=\langle 3|\mathbf{u}_i\cdot\mathbf{n}|^2-1\rangle/2$, with $\mathbf{u}_i$ and $\mathbf{n}$ as the orientation of particle i and the nematic director, respectively [12]. The smectic order is characterized by a nonhomogeneous density profile $\pi(z)$ with z along the nematic director. Interestingly, we find that the barrier height in smectic LC phases is higher for aligned hard rods than for freely rotating rods at the same packing fraction, i.e., we find $U_0=5.1k_BT$ at $\eta=0.508$ ($P^*=3.7$) for aligned rods, which should be compared with $U_0=3.5k_BT$ for freely rotating rods, and $U_0=7.8k_BT$ at $\eta=0.557$ ($P^*=4.8$) for parallel rods to be compared with $U_0=7.5k_BT$. The difference in barrier height decreases with increasing pressure, and we expect that it tends to zero upon approaching the Sm-K transition, where the freely rotating rods become more and more aligned. In summary, the intralayer diffusion is more delayed in the case of perfectly aligned rods, due to an increase in layer-to-layer order, resulting in significantly higher potential-energy barriers.

Barrier-free diffusion pathways can be observed even at high densities as a result of screw dislocations. Such structural defects create helical connections between neighboring smectic layers where the rods diffuse as in the nematic phase [26]. It is not an easy task to model screw dislocations in computer simulations as these are not compatible with periodic boundary conditions. Slip boundary conditions may overcome this complication [27].

To study the non-Gaussian behavior of the layer-to-layer diffusion, we computed the following non-Gaussian parameter [28]:

$$\alpha_{2,z}(t) = \frac{\langle \Delta z(t)^4 \rangle}{3\langle \Delta z(t)^2 \rangle^2} - 1, \tag{1}$$

where $\Delta z(t)=z(t_0+t)-z(t_0)$ is the displacement of the rods in the z direction in the time interval starting at t_0 and ending at t_0+t and $\langle \ldots \rangle$ denotes an ensemble average over all particles and initial time t_0. For the in-layer diffusion, a similar non-Gaussian parameter, $\alpha_{2,xy}(t)$, can be computed. In Fig. 4, we show $\alpha_{2,z}(t)$ at different pressures. This parameter quantifies the deviation from the Gaussian behavior of the probability density function for single-particle diffusion. At short times, the particles are freely diffusing as the trapping cage formed by the surrounding neighbors is not reached yet and, hence, $\alpha_{2,z}$ is basically zero. At long times, the system enters the diffusive regime and the non-Gaussian parameter tends to zero. At intermediate times, the motion of each particle is

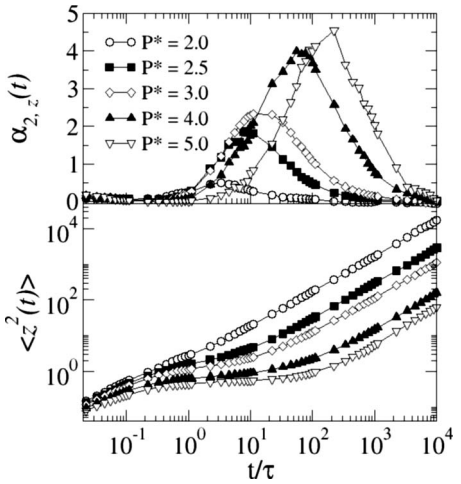

FIG. 4. Non-Gaussian parameter $\alpha_{2,z}(t)$ and mean-square displacement in the direction parallel to the nematic director calculated at the pressures indicated in the top frame.

hampered by its neighbors and becomes subdiffusive. In this time interval, $\alpha_{2,z}$ is nonvanishing, indicating the development of dynamical heterogeneities. Additionally, we find that the peak height of $\alpha_{2,z}(t^*)$ at t^* increases and moves to larger values of t^* upon increasing the packing fraction as the time for the particles to escape out of their cage increases. We also plot the mean-square displacement (MSD) $\langle z^2(t)\rangle$ in Fig. 4 for the same state points. The MSD show a clear cage-trapping plateau, which becomes more pronounced upon increasing pressure. The time t^* at which $\alpha_{2,z}$ displays a maximum corresponds to the end of the plateau observed in the MSD as can be observed clearly in Fig. 4.

Interestingly, non-Gaussian dynamics due to cage-escape processes have also been observed in single-particle diffusion in periodic external potentials [29], 2D liquids [30], cluster crystals [31], but also in glasses [32–35]. In particular, it was shown that the time to escape out of a cage increases because cage rearrangement (or recaging) involves a larger number of particles [32–35] upon approaching the glass transition. $\alpha_{2,xy}(t)$ (not shown here) does not deviate significantly from zero. At the highest pressure studied, the peak is lower than 0.2, confirming that the in-layer relaxation dynamics is (nearly) diffusive. The behavior of the non-Gaussian parameter $\alpha_{2,z}$ is consistent with the theoretical predictions in systems of infinitely long parallel hard rods [18] and with the simulation results of freely rotating hard rods [12] although the latter exhibit higher peaks especially close to the smectic-to-crystal transition. Stronger deviations have been observed in colloidal systems with short-range attractions when approaching the gel transition [36] or in permanent gels where *static* heterogeneities give rise to a plateau at long times (i.e., the non-Gaussian parameter does not vanish) [4,37]. Glass transitions, by contrast, are usually characterized by weaker deviations [33,35].

The periodic shape of the effective potential implies a *hopping-type* diffusion in the direction of $\hat{n}$, with the rods rattling around in a given layer until they overcome the free-energy barrier shown in Fig. 3 and jump to a neighboring layer. We quantify this layer-to-layer diffusion by calculating

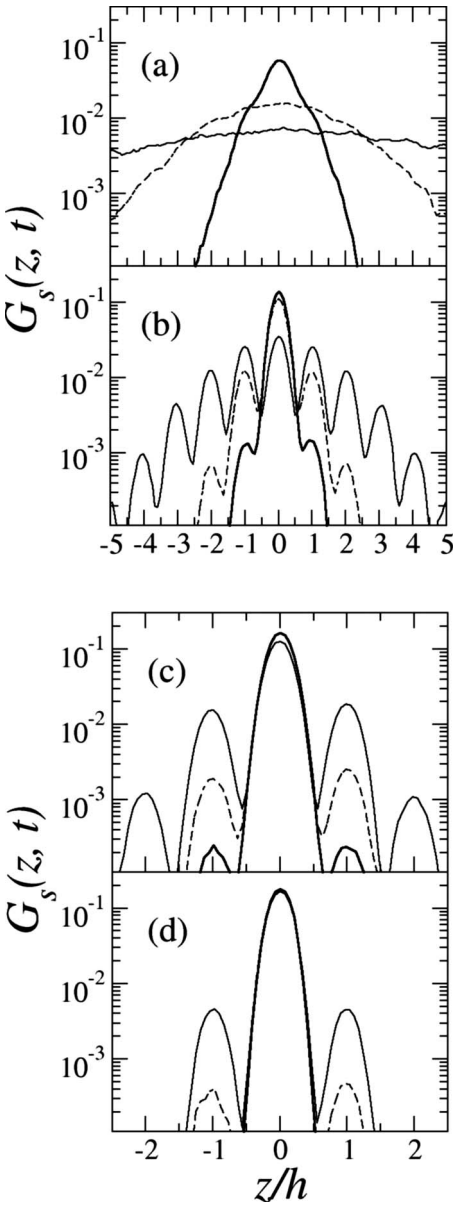

FIG. 5. Self-part of the Van Hove function $G_s(z,t)$ at $t/\tau=10$ (thick solid lines), $t/\tau=100$ (dashed lines), and $t/\tau=1000$ (solid lines) for pressure (a) $P^*=2.0$, (b) 3.0, (c) 4.0, and (d) 5.0.

the self-part of the Van Hove correlation function (VHF) [38] defined as

$$G_s(z,t) = \frac{1}{N}\left\langle \sum_{i=1}^{N} \delta(z - [z_i(t_0+t) - z_i(t_0)]) \right\rangle, \qquad (2)$$

where δ is the Dirac delta function. $G_s(z,t)$ measures the probability distribution for the z displacements of the rods at time t_0+t, given their z positions at t_0. In Fig. 5, the self-VHF is presented as a function of z at $P^*=2.0$ to 5.0. At $P^*=3.0$ to 5.0, we observe the appearance of peaks at distances that correspond to the center of the smectic layers in the z direction. No peaks are observed at $P^*=2.0$, where the barrier height $(0.2k_BT)$ of the effective potential for the layer-to-layer diffusion is sufficiently small that there is no

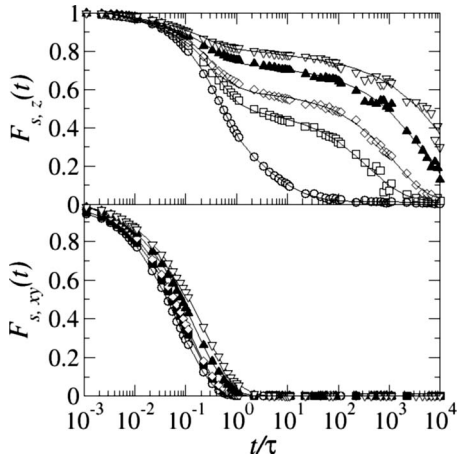

FIG. 6. Self-intermediate scattering function $F_s(t)$ for the structural relaxation in the z (top) and xy (bottom) direction at $P^*=2.0$ (○), 2.5 (■), 3.0 (◇), 4.0 (▲), and 5.0 (▽). The solid lines are fits.

hopping-type diffusion between neighboring layers. As a result, the discontinuous diffusion observed in strong smectic phases, with the particles occupying quasidiscretized positions, is substituted by a quasicontinuous Gaussian diffusion for weak smectic phases. At long times, less and less particles are still at their original positions, and consequently, the profiles of the VHF become almost constant in a nematic phase or periodically peaked in a smectic phase. The presence of peaks at distances of neighboring layers for small to intermediate pressures show that a significant number of particles have displaced a long distance even at short times. These fast-moving particles contribute to the heterogeneous dynamics of the system and affect its structural relaxation. In recent simulations of smectic phases of freely rotating hard rods, it was shown that the fast-moving particles form string-like clusters which exhibit cooperative motion [12]. We believe that this result is still valid if the orientational degrees of freedom are frozen out, but further investigation is needed to address this point in more detail.

Finally, we also study the structural relaxation by calculating the self-part of the intermediate scattering function:

$$F_s(t) = \langle \exp[i\mathbf{q} \cdot \Delta\mathbf{r}(t)] \rangle \tag{3}$$

at wave vectors $\mathbf{q}D=(0,0,q_z)$ and $(q_x,q_y,0)$, with $q_z \simeq 1$ and $(q_x^2+q_y^2)^{1/2} \simeq 6$, which correspond to the main peaks of the static structure factor. $\Delta\mathbf{r}(t)$ is the displacement of a particle in the time interval t. Results at pressures $P^*=2.0$, 3.0, and 4.0 are shown in Fig. 6. For the pressure range $P^*=2.5-5.0$, the interlayer dynamics shows a significantly slow relaxation which is characterized by a two-step decay. In the first step, which is relatively fast, each rod rattles around its original position without feeling the presence of the surrounding neighbors. We detect an exponential decay of $F_{s,z}(t)$ toward a plateau whose height and time extension increase with pressure as also observed for colloidal glasses [3]. The plateau establishes the beginning of the cage regime, where the particles start to interact with their nearest neighbors which form a temporary cage for the particle. The following step takes place at much longer times (note the logarithmic scale of Fig. 6) and marks the escape from the cage regime. The second decay of $F_{s,z}$ is well fitted by a stretched exponential function of the form $\exp[(t/tr)^{\beta}]$, where $\beta \simeq 0.6$ and t_r is the time at which the intermediate scattering function decays to e^{-1}. The stretched exponential form of the relaxation decay at long times confirms the heterogeneous nature of the inter layer dynamics. In Fig. 7, the relaxation time is given as a function of the packing fraction and fitted with a power law covering four time decades in a density interval spanning from the N-Sm to the Sm-K transition. At $P^*=2.0$, we still observe an initial exponential decay at short times and a stretched exponential decay at long times, but it is very hard to detect a plateau (if any) due to the weak smectic character of the bulk phase and, hence, to the weak permanent background barriers (see Fig. 3). Nevertheless, there might be a discontinuity between two separated relaxation regimes since $F_{s,z}$ cannot be fitted by a single scaling law.

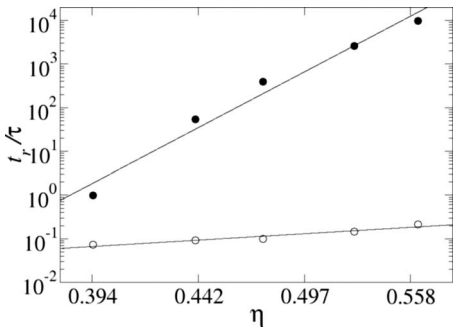

FIG. 7. Relaxation time t_r/τ as a function of packing fraction η. The solid and empty circles refer to the interlayer and in-layer relaxation, respectively. The solid lines are power-law fits of the type $t_r/\tau \propto \eta^a$, with $a=25.2$ and 2.89 for the interlayer and in-layer relaxation, respectively.

By contrast, the in-layer relaxation is very fast and occurs in a single step. As can be observed in Fig. 7, the relaxation time, which covers basically half a time decade, does not change significantly as a function of density. Interestingly, the long time decay of $F_{s,xy}$, which is exponential at short times, is also fitted by a stretched exponential function with $\beta \simeq 0.7$ at long times. This behavior is unusual for simple fluids, where a single exponential decay is observed, and can also not be associated with that of a supercooled liquid as the characteristic cage-trapping plateau is absent. However, the in-layer dynamics in smectic liquid crystals is similar to that of low-density supercooled liquids which do not display a plateau but only a stretched exponential relaxation at long times [39].

IV. CONCLUSIONS

In conclusion, we have studied using computer simulations the diffusion of perfectly aligned rodlike particles in smectic liquid-crystal phases, where the interlayer dynamics exhibits a non-Gaussian rattling-and-jumping-type diffusion due to the simultaneous presence of temporary cages and permanent barriers. The caging due to the mutual trapping of neighboring particles, slows down the diffusion, and the cor-

responding relaxation time depends strongly on the packing of the system. The presence of periodic permanent barriers with a height that increases with increasing density are intrinsically associated to the layered structure of the smectic phase and determine the hopping-type layer-to-layer diffusion. As detected in out-of-equilibrium colloidal systems, such as supercooled liquids, we found that in a given time interval some particles displace longer distances than the average, giving rise to a remarkable heterogeneous dynamics which results in significant deviations from Gaussian behavior. We quantified these heterogeneities by computing (1) the non-Gaussian parameter $\alpha_{2,z}(t)$, which significantly deviates from zero at high volume fractions; (2) the self-part of the van Hove functions, whose long tails give clear evidence of the presence of *fast* particles even at short times; (3) the mean-square displacement, which exhibits a plateau quantifying the average lifetime of the transient cages; and (4) the self-part of the intermediate scattering function, which characterizes the relaxation decay of the system. In the complete range of stability of the smectic phase, we observed a very slow interlayer structural relaxation which spans over four time decades from the N-Sm to the Sm-K transition. We note that caging as well as the permanent barrier both contribute to the non-Gaussian dynamics [29]. The in-layer relaxation dynamics is very fast but does not show an exponential decay at long times as it would be expected for simple liquids. The observed stretched-exponential decay corresponds to that of a low-density supercooled liquid where the cage effect is not sufficiently strong to yield a cage-trapping plateau.

We observed qualitative agreement with the dynamics of freely-rotating hard rods [12], but we do find some quantitative deviations in the non-Gaussian behavior, mainly, caused by the huge differences in the height of the potential-energy barriers. To be specific, the height of the barrier for aligned rods tends to zero at the continuous N-Sm transition, while it remains finite in the case of the first order N-Sm transition of freely rotating rods, which changes the dynamics significantly. Strings of clusters which exhibit cooperative motion have been found in systems of freely rotating hard rods [12], and we expect that they should be observed also when the orientational degrees of freedom are frozen out. Other transient heterogeneities, which alter the order of the smectic structure, may arise from localized defects, such as stacking faults and dislocations. The small size of our system and the periodic boundary conditions prevent the formation of defects. However, one could indeed expect that some types of structural defects, such as screw dislocations, facilitate the layer-to-layer diffusion by allowing for barrier-free nematic-like "fast tracks" through the smectic layers [26].

ACKNOWLEDGMENT

This work was financed by a NWO-VICI grant.

[1] W. Kob, C. Donati, S. J. Plimpton, P. H. Poole, and S. C. Glotzer, Phys. Rev. Lett. **79**, 2827 (1997).
[2] L. Berthier, G. Biroli, J.-P. Bouchaud, L. Cipelletti, D. El Masri, D. L'Hôte, F. Ladieu, and M. Pierno, Science **310**, 1797 (2005).
[3] G. Brambilla, D. El Masri, M. Pierno, L. Berthier, L. Cipelletti, G. Petekidis, and A. B. Schofield, Phys. Rev. Lett. **102**, 085703 (2009).
[4] T. Abete, A. de Candia, E. Del Gado, A. Fierro, and A. Coniglio, Phys. Rev. E **78**, 041404 (2008).
[5] A. M. Puertas, M. Fuchs, and M. E. Cates, J. Chem. Phys. **121**, 2813 (2004).
[6] R. Richert, J. Non-Cryst. Solids **172–174**, 209 (1994).
[7] A. Lefèvre, L. Berthier, and R. Stinchcombe, Phys. Rev. E **72**, 010301(R) (2005); A. S. Keys, A. R. Abate, S. C. Glotzer, and D. J. Durian, Nat. Phys. **3**, 260 (2007).
[8] R. Lefort, D. Morineau, R. Guegan, M. Guendouz, J. M. Zanotti, and B. Frick, Phys. Rev. E **78**, 040701(R) (2008).
[9] Q. Ji, R. Lefort, R. Busselez, and D. Morineau, J. Chem. Phys. **130**, 234501 (2009).
[10] H. Cang, J. Li, V. N. Novikov, and M. D. Fayer, J. Chem. Phys. **118**, 9303 (2003).
[11] S. D. Gottke, D. D. Brace, H. Cang, B. Bagchi, and M. D. Fayer, J. Chem. Phys. **116**, 360 (2002).
[12] A. Patti, D. El Masri, R. van Roij, and M. Dijkstra, Phys. Rev. Lett. **103**, 248304 (2009).
[13] P. G. de Gennes and J. Prost, *The Physics of Liquid Crystals* (Clarendon, Oxford, 1993).
[14] L. Frunza, S. Frunza, H. Kosslick, and A. Schönhals, Phys. Rev. E **78**, 051701 (2008).
[15] R. Guégan, D. Morineau, R. Lefort, A. Moréac, W. Béziel, M. Guendouz, J.-M. Zanotti, and B. Frick, J. Chem. Phys. **126**, 064902 (2007).
[16] I. Furó and S. V. Dvinskikh, Magn. Reson. Chem. **40**, S3 (2002).
[17] M. P. Lettinga and E. Grelet, Phys. Rev. Lett. **99**, 197802 (2007).
[18] M. Bier, R. van Roij, M. Dijkstra, and P. van der Schoot, Phys. Rev. Lett. **101**, 215901 (2008).
[19] A. Stroobants, H. N. W. Lekkerkerker, and D. Frenkel, Phys. Rev. Lett. **57**, 1452 (1986).
[20] J. A. C. Veerman and D. Frenkel, Phys. Rev. A **43**, 4334 (1991).
[21] M. Doi and S. F. Edwards, *The Theory of Polymer Dynamics* (Clarendon Press, Oxford, 1994).
[22] V. Pryamitsyn and V. Ganesan, J. Chem. Phys. **128**, 134901 (2008).
[23] F. Volino, A. J. Dianoux, and A. Heidemann, J. Phys. (France) Lett. **40**, 583 (1979).
[24] R. M. Richardson, A. J. Leadbetter, D. H. Bonsor, and G. J. Krüger, Mol. Phys. **40**, 741 (1980).
[25] J. S. van Duijneveldt and M. P. Allen, Mol. Phys. **90**, 243 (1997).
[26] Robin L. Blumberg Selinger, Phys. Rev. E **65**, 051702 (2002).
[27] J. V. Lill and J. Q. Broughton, Phys. Rev. B **63**, 144102 (2001).

[28] A. Rahman, Phys. Rev. **136**, A405 (1964).
[29] B. Vorselaars, A. V. Lyulin, K. Karatasos, and M. A. J. Michels, Phys. Rev. E **75**, 011504 (2007).
[30] M. M. Hurley and P. Harrowell, J. Chem. Phys. **105**, 10521 (1996).
[31] A. J. Moreno and C. N. Likos, Phys. Rev. Lett. **99**, 107801 (2007).
[32] C. Donati, J. F. Douglas, W. Kob, S. J. Plimpton, P. H. Poole, and S. C. Glotzer, Phys. Rev. Lett. **80**, 2338 (1998).
[33] E. R. Weeks and D. A. Weitz, Phys. Rev. Lett. **89**, 095704 (2002).
[34] Eric R. Weeks, J. C. Crocker, Andrew C. Levitt, Andrew Schofield, and D. A. Weitz, Science **287**, 627 (2000).
[35] W. K. Kegel and A. van Blaaderen, Science **287**, 290 (2000).
[36] A. M. Puertas, M. Fuchs, and M. E. Cates, Phys. Rev. E **67**, 031406 (2003).
[37] T. Abete, A. de Candia, E. Del Gado, A. Fierro, and A. Coniglio, Phys. Rev. Lett. **98**, 088301 (2007).
[38] J. P. Hansen and I. R. McDonald, *Theory of Simple Liquids* (Academic, London, 1986).
[39] D. El Masri, G. Brambilla, M. Pierno, G. Petekidis, A. B. Schofield, L. Berthier, and L. Cipelletti, J. Stat. Mech.: Theory Exp. (2009), P07015.